Morphotectonic Analysis of Maharlu area, Zagros, Iran

Babak Samani, Naeim Matin, Abbas Charchi

***Abstract*— The study area has been located in the Zagros Mountains, south west Iran. Ghare, Maharlu and Sarvestan faults are the most important faults in the area. These faults form the southern, northern and eastern boundaries of the Maharlu plain respectively. Kinematic mechanisms of these faults are the important effects in the structural evolution of the Maharlu Lake. The Geomorphic indices including stream length–gradient index (SL), mountain front sinuosity (Smf), valley floor width to valley height ratio (Vf), basin shape index (Bs), and Basin asymmetry factor (Af) have been evaluated for determination of various tectonic activities in the area. Based on the quantitative amounts of each index, density distribution map of various parameters were prepared along the mentioned faults. In order to understand the amounts of tectonic activity, each of these indices were classified into three standards groups. Results of the amounts of tectonic activity indices (Iat) and overlied data layer show more tectonic activity in the eastern parts and especially in the contacts of Maharlu and Sarvestan faults. Morphotectonic comparisons of faults reveal that the sarvestan fault and the central part of Ghare faults are more active than other parts of the study are.**

***Index Terms*—** Morphotectonic, Geomorphic indices, Zagros Mountains, Iran

I. INTRODUCTION

Iran has been divided into several structural units. Zagros Mountain is one of the main structural units that consists a fold-and-thrust belt which located in the southwestern Iran. The Zagros fold-and-thrust belt is resulted due to the late Cretaceous collision between Arabian and Iran plates (Navabpour and Barrier, 2012). The Zagros fold-and-thrust belt as a part of the Alpine-Himalaya mountain chain is a well-characterize asymmetric orogenic belt (Alavi, 1994). This belt is one of the youngest orogen in the word that is active and today is under suffer a shortening with median rate about 20 mm/yr-1 (Jackson and McKenzie, 1984) in result of collision between Arabian and central Iranian plates (Berberian et al., 1982; Berberian, 1983; Berberian and King, 1981). Today features of the Zagros Mountain are related to reaction of both tectonic and weathering possesses. Active tectonics can be considered as the main factor contributing to rock uplift and relief in mountain areas, and result from the interaction of tectonic and surface processes (Andermann and Gloaguen, 2009; Azor et al., 2002; Keller and Pinter, 2002; Mahmood and Gloaguen, 2012; Pérez-Peña et al., 2010). This interaction is a key element in tectonic geomorphology investigations for understanding Earth's dynamic surface (Burbank and Anderson, 2012). Geomorphological studies of active tectonics in the late Pleistocene and Holocene are important to evaluate tectonically active areas such as the Zagros (Keller and Pinter, 2002). Digital Elevation Models (DEMs) make better and faster analysis of topographic changes resulting from the competition between tectonic and surface processes (Azañón et al., 2012; Farr and Kobrick, 2000; Grohmann, 2004; Grohmann et al., 2007; Troiani and Della Seta, 2008). The information about geomorphic indicators of active tectonics can be retrieved through analysis of DEMs and quantification of geomorphic indices. 3D analyst tools contain geographic information systems (GIS) and morphometric analyses can provide helpful information on this topic.

Several systematic investigations have been conducted to study the effect of active tectonics on the geomorphic characteristics of landscapes using geomorphic indices in various tectonically active areas or fault zones (Giaconia et al., 2012; Joshi et al., 2013; Keller and DeVecchio, 2012). This paper expressed quantitative geomorphological method to a local in the Zagros to assessment related rates of active tectonic. We studied five geomorphic indices: the Basin shape (Bs), Mountain-front sinuosity (Smf) Stream Length-gradient index (SL), Ratio of valley floor width to valley heigh (Vf), and Asymmetry factor (Af). Finally we analyzed an index (Iat) to determine relationship between active tectonic in these mentioned indices. This type of methodology has been found to be useful in different tectonically active areas such as Narmada–Son Fault, Western India (Joshi et al., 2013), southwestern Sierra Nevada of Spain (El Hamdouni et al., 2008), The Mediterranean coast of Spain (Silva et al., 2003).

II. REGIONAL GEOLOGICAL SETTING

The active Zagros fold-thrust belt located on the northeastern margin of the Arabian plate, on Precambrian basement (Berberian, 1994). The Zagros Fold-Thrust Belt contains an 8–14 km thick Cambrian-Recent sedimentary succession that rests on Precambrian metamorphic basement (Samani and Faghih, 2014). These sedimentary rocks were deposited on a platform that was relatively stable from the Cambrian until the collision between the Arabian and Iranian plates in the Late-Cretaceous to Tertiary (Berberian and King, 1981; Falcon, 1974; Takin, 1972). Shortening across the Zagros Fold-and-Thrust Belt is estimated to be about 30–85 km

Babak Samani, Faculty of Earth sciences, Shahid Chamran University of Ahvaz, Iran. (samani.babak@gmail.com).
Naeim Matin, Faculty of Earth sciences, Shahid Chamran University of Ahvaz, Iran.
Abbas Charchi, Faculty of Earth sciences, Shahid Chamran University of Ahvaz, Iran.

(Blanc et al., 2003; Falcon, 1974; McQuarrie, 2004), and thought to have occurred by thrusting and folding above a number of décollement horizons (McQuarrie, 2004).
Shortening in the basement occurs dominantly by faulting. The thick Cambrian Hormuz Salt, at the base of the sedimentary succession, and other evaporate horizons (e.g. the Dashtak and Gachsaran Formations) within the succession (Berberian and King, 1981; Sepehr and Cosgrove, 2005; Talebian and Jackson, 2002), prevented these basement faults from reaching the surface. The Zagros Fold-and-Thrust belt mainly consists of asymmetrical folds, which form a 200–300 km wide series of ranges extending for about 1800 km along strike from eastern Turkey to southeastern Iran, in the Strait of Hormuz. The study area is located in the Maharlu area, 100 km southeastern of Shiraz. Figure 1, shows the geological map of the study area. Maharlu, Ghare and sarvestan faults are the main fault system in the area. In this paper tectonic activity along the main faults was evaluated with application of morphometric indices.

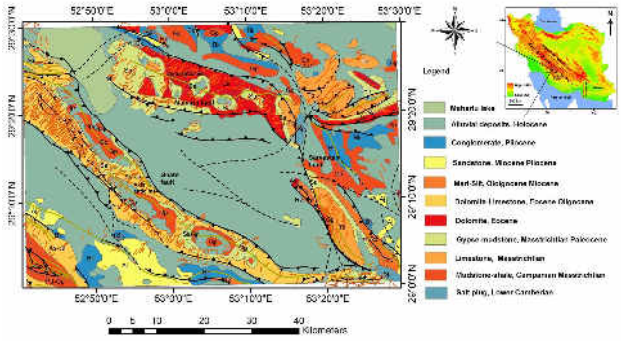

Figure 1: Geological map of the study area

III. DISCOSSION

Morphometry is denoting as quantitative measurement of landform shape. Geomorphic indices help to measurement and assessment tectonic activity. Most of the geomorphic and morphometric parameters used in this study were developed by Hack (1973), Bull and McFadden (1977), Rantsman (1979), Wells et al. (1988), Keller and Pinter (1996), Silva et al. (2003) and El-Hamdouni et al. (2008). Main parameters used in these analyses quantify the tectonic activity; include stream-gradient index (SL), drainage basin asymmetry (Af), valley floor width–valley height ratio (Vf), drainage basin shape (Bs) and mountain-front sinuosity (Smf). The geomorphological and morphometric analyses were carried out using 1:25000 scale topographic maps and digital elevation models.

IV. STREAM LENGTH-GRADIEND INDEX (SL)

According to Keller and Pinter (1996) the stream length-gradient index is calculated for the area and defined as:

$$SL = \frac{\Delta H}{\Delta L} \times (L)$$

SL is the stream length-gradient index, ΔH is relocation in elevation, ΔL is change in distances, indeed ΔH/ΔL is gradient of the reach and L is the length from point of the reach to highest point in the stream. This index calculated in situations of study area that main watersheds interrupt mountain dominant trend of main faults. Figure 2 shows some stream profiles across the Maharlou, Ghare and Sarvestan faults.

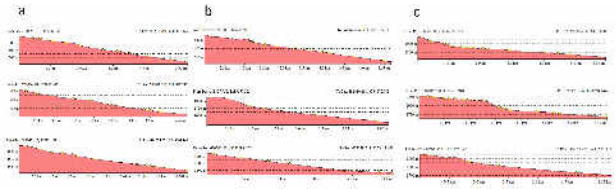

Figure 2: a, b and c, some longitudinal stream profiles across Maharlu, Ghare and Sarvestan faults

SL value was calculated along the faults in the points of transversal drainages. Table 1 shows the calculated SL value for all three faults. Finally the SL density distribution map was prepared based on IDW model (Fig, 3). The SL amounts were classified based on (El Hamdouni et al., 2008) for understanding the active tectonic variations in the area (Fig, 4). The values classified in three classification: 1 (SL≥500) (high active tectonic), 2 (300≤SL<500) (median active tectonic) and 3 (SL<300) (low active tectonic) (El Hamdouni et al., 2008).

Table 1: Values and classes of SL index in the area along Maharlu, Ghare and Sarvestan faults

Maharlu Fault			Ghare Fault			Sarvestan Fault		
No.	Sl	Class	*No.*	Sl	Class	No.	Sl	Class
1	240	3	*9*	120	3	**18**	55.46	3
2	243.6	3	*10*	153.75	3	**19**	103.68	3
3	188.15	3	*11*	73.18	3	**20**	650.89	1
4	221	3	*12*	250.8	3	**21**	204.48	3
5	127.93	3	*13*	256.66	3	**22**	42.85	3
6	98.57	3	*14*	115.58	3	**23**	162.13	3
7	518.18	1	*15*	98.66	3	**24**	202.66	3
8	15.4	3	*16*	31.9	3			
			17	250.51	3			

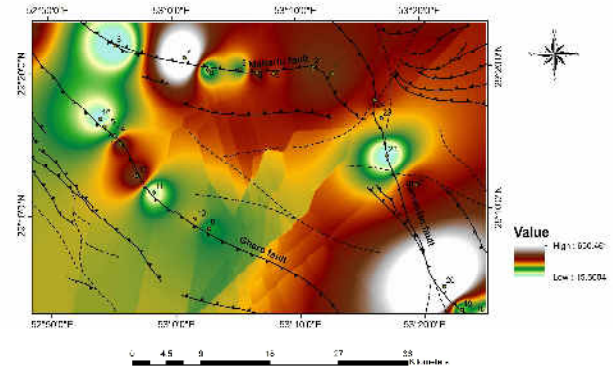

Figure 3: Density distribution map of SL index values

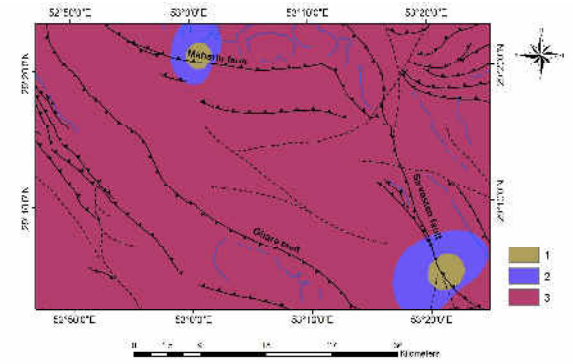

Figure 4: Distribution of SL classified map

V. RATIO OF VALLEY FLOOR WIDTH TO VALLEY HEIGHT (VF)

According to Keller and Pinter (1996) the ratio of valley floor width to valley height is calculated for the area and defined as:

$$Vf = \frac{2Vfw}{(Eld - Esc) + (Erd - Esc)}$$

Vfw is the width of the valley, Eld is the elevation of the left valley, Erd is the elevation of the right valley and Esc is the elevation of the stream channel (Silva et al., 2003). Figure 5 shows some valleys profiles across the Maharlu, Ghare and Sarvestan faults.

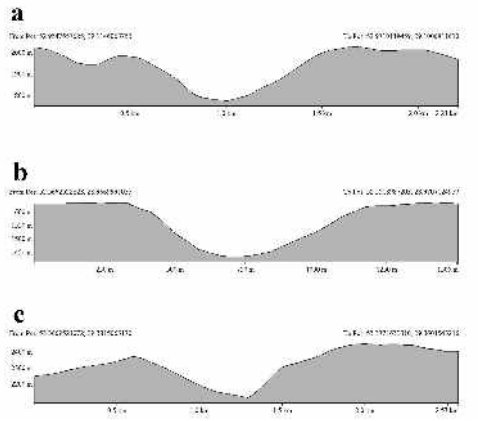

Figure 5: a, b and c, some longitudinal valleys profiles across Ghare, Maharlu and Sarvestan, faults

Vf value was calculated along the faults in the points of transversal valleys. Table 2 shows the calculated Vf value for all three faults. Finally the Vf density distribution map was determined based on IDW model (Fig, 6). The Vf amounts were classified based on (El Hamdouni et al., 2008) for understanding the active tectonic variations in the area (Fig, 7). The values classified in three classification: 1 (Vf≤ 0.5) (high active tectonic), 2 (0.5≤Vf<1.0) (median active tectonic) and 3 (Vf≥ 1) (low active tectonic) (El Hamdouni et al., 2008). This index compared width of valleys floor respect to altitude of valley wall, actually dissociation between valleys with a U shape (wide valleys) to valleys with a V shape (tight valleys), (Silva et al., 2003). Valleys U shape principally have more values of Vf to V shape valleys have few rather values.

Table 2: Values and classes of Vf index in the area along Ghare, Sarvestan and Maharlu faults

Ghare Fault			Sarvestan Fault			Maharlu Fault		
No.	Vf	Class	*No.*	Vf	Class	*No.*	Vf	Class
1	2.18	3	*6*	0.39	1	*14*	2.12	3
2	1.70	3	*7*	0.72	2	*15*	9.09	3
3	4.28	3	*8*	4.16	3	*16*	34	3
4	10	3	*9*	18	3	*17*	0.87	2
5	8	3	*10*	0.46	1	*18*	3.33	3
			11	4.40	3			
			12	4.50	3			
			13	0.17	1			

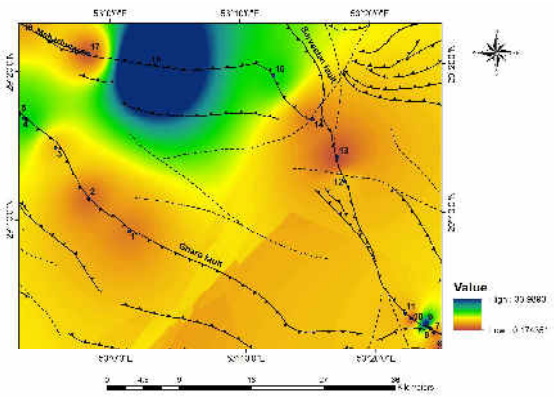

Figure 6: Density distribution map of Vf index values

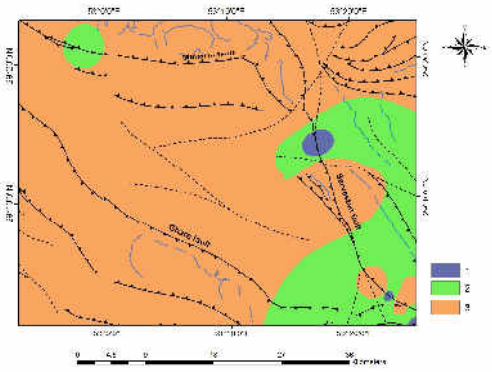

Figure 7: Distribution of Vf classified map

VI. Basin shape (BS) index

The drainage basin shape index quantifies the planim shape of a basin to the distance between the two most distal points in the basin (Ramirez-Herrera, 1998) and ca expressed as:

$$BS = \frac{BL}{BW}$$

where Bl is the length of a basin measured from the high point to the most distant drainage divide, and Bw is the width of a basin measured at its widest point across the basin. B draining tectonically active areas are more elongated and become more circular with the cessation of uplift (Bull McFadden, 1977, Ramirez-Herrera, 1998; Mahmood and Gloaguen, 2012). For measuring the basin shape ir watersheds were extracted in the Global Mapper software by using DEMs of area (Fig, 8).

The Bs value was calculated along the faults in the diff sub-basins (Fig, 8). Table 3 shows the calculated Bs value for all sub-basins. Finally the Bs density distribution map prepared based on IDW model (Fig, 9). The Bs amounts were classified based on (El Hamdouni et al., 2008) understanding the active tectonic variations in the area (Fig, 10). The values classified in three classification: 1 (B (high active tectonic), 2 (3-Apr) (median active tectonic) and 3 (BS<3) (low active tectonic) (El Hamdouni et al., 200

Table 3: Values and classes of Bs index in the area along Sarvestan, Maharlu, and Ghare faults

Sarvestan Fault			Maharlu Fault			Ghare Fault		
No.	Bs	Class	*No.*	Bs	Class	*No.*	Bs	Class
1	3.53	2	*27*	4.95	1	*60*	8.38	1
2	1.94	3	*28*	3.77	2	*61*	2.77	3
3	3.46	2	*29*	3.46	2	*62*	3.51	2
4	1.94	3	*30*	2.26	3	*63*	10.8	1
5	1.92	3	*31*	1.33	3	*64*	1.99	3
6	2.21	3	*32*	1.99	3	*65*	1.49	3
7	4.20	1	*33*	3.93	2	*66*	3.39	2
8	2.73	3	*34*	3.87	2	*67*	2.48	3
9	6.49	1	*35*	2.49	3	*68*	2.99	3
10	2.65	3	*36*	4.88	1	*69*	5.15	1
11	5.15	1	*37*	2.02	3	*70*	4.24	1
12	4.46	1	*38*	1.65	3	*71*	3.64	2
13	4.00	1	*39*	3.04	2	*72*	2.51	3
14	5.77	1	*40*	1.65	3	*73*	1.48	3
15	6.19	1	*41*	1.64	3	*74*	5.61	1
16	3.83	2	*42*	3.37	2	*75*	2.06	3
17	3.50	2	*43*	6.49	1	*76*	1.68	3
18	2.91	3	*44*	3.62	2	*77*	0.99	3
19	5.53	1	*45*	3.03	2	*78*	1.95	3
20	2.94	3	*46*	1.70	3	*79*	1.31	3
21	1.77	3	*47*	4.79	1	*80*	4.60	1
22	4.41	1	*48*	4.96	1	*81*	1.47	3
23	2.61	3	*49*	3.35	2	*82*	0.97	3
24	2.93	3	*50*	1.01	3	*83*	4.36	1
25	4.61	1	*51*	2.01	3	*84*	1.96	3
26	0.97	3	*52*	2.00	3	*85*	2.66	3
			53	4.48	1	*86*	2.01	3
			54	3.49	2	*87*	4.43	1
			55	2.91	3	*88*	4.36	1
			56	1.49	3	*89*	5.85	1
			57	3.70	2	*90*	4.54	1
			58	1.67	3	*91*	6.91	1
			59	3.40	2	*92*	2.63	3
						93	3.11	2
						94	1.99	3
						95	1.97	3
						96	1.97	3
						97	1.01	3
						98	4.43	1
						99	2.45	3
						100	1.57	3
						101	1.50	3
						102	0.25	3
						103	3.42	2
						104	2.11	3
						105	11.5	1
						106	4.11	1
						107	1.93	3
						108	1.35	3
						109	1.63	3

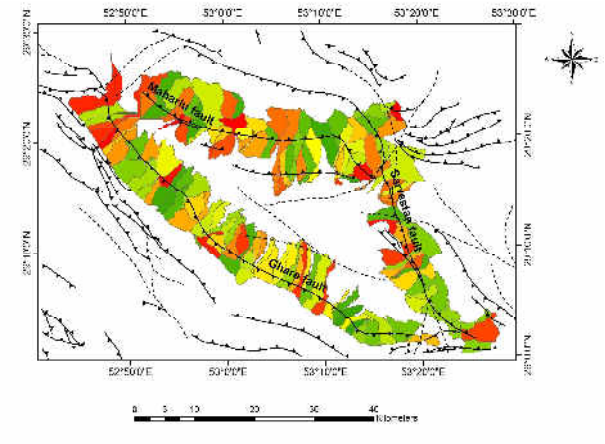

Figure 8: Subbasins of the Maharlu area along Ghare, Maharlu and Sarvestan faults

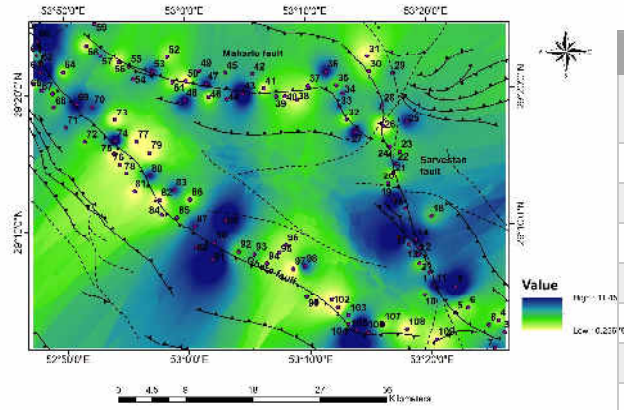

Figure 9: Density distribution map of Bs index values

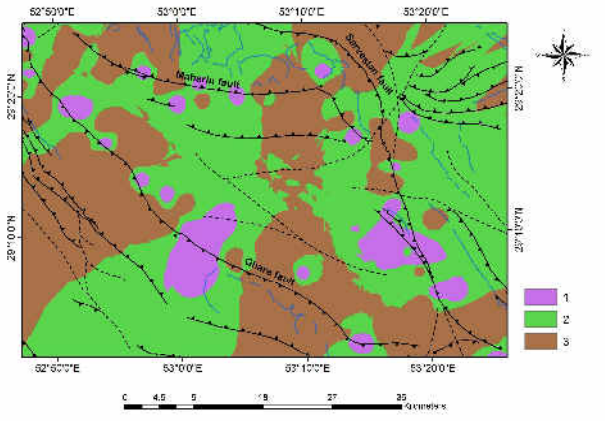

Figure 10: Distribution of Bs classified map

VII. Mountain Front Sinuosity (Smf) Index

According to Bull and McFadden (1977) and Keller and Pinter (1996) index of mountain front sinuosity is calculated for the area and defined as:

$$Smf = \frac{Lmf}{Ls}$$

Smf is defined as the ratio of the length of the mountain front to straight line of mountain front, (Lmf) is the length of the mountain front in the length of piedmont , (Ls) is the straight line to the mountain front (Bull and McFadden, 1977; Keller and Pinter, 2002). If mountain fronts be relative to active tectonics and straight approximately uplift, this index has low Smf values, If rate of uplift be decreased, erosion process cause of done more erosion mountain fronts and eventually due to increase Smf values (Keller and Pinter, 1996).

Smf value was calculated along the faults in the mountain front. Table 4 shows the calculated Smf value for all three faults. Finally the Smf density distribution map was prepared based on IDW model (Fig, 11). The Smf amounts were classified based on (El Hamdouni et al., 2008) for understanding the active tectonic variations in the area (Fig, 12). The values classified in three classification: 1 (Smf<1.1) (high active tectonic), 2 (1.1≤Smf≤1.5) (median active tectonic) and 3 (Smf>1.5) (low active tectonic) (El Hamdouni et al., 2008).

Table 4: Values and classes of Bs index in the area along Ghare, Sarvestan and Maharlu faults

Ghare Fault			Sarvestan Fault			Maharlu Fault		
No.	Smf	Class	*No.*	Smf	Class	*No.*	Smf	Class
1	1.80	3	*14*	1.51	2	*24*	1.10	2
2	1.91	3	*15*	1.98	3	*25*	1.29	2
3	1.45	2	*16*	1.06	1	*26*	1.34	2
4	1.21	2	*17*	1.00	1	*27*	1.60	3
5	1.42	2	*18*	1.18	2	*28*	1.19	2
6	1.05	1	*19*	1.32	2	*29*	1.75	3
7	1.41	2	*20*	3.78	3	*30*	1.16	2
8	1.99	3	*21*	1.00	1	*31*	1.63	3
9	1.16	2	*22*	1.91	3	*32*	2.60	3
10	1.72	3	*23*	2.67	3	*33*	3.02	3
11	1.09	1				*34*	1.88	3
12	1.09	1				*35*	2.74	3
13	1.09	1						

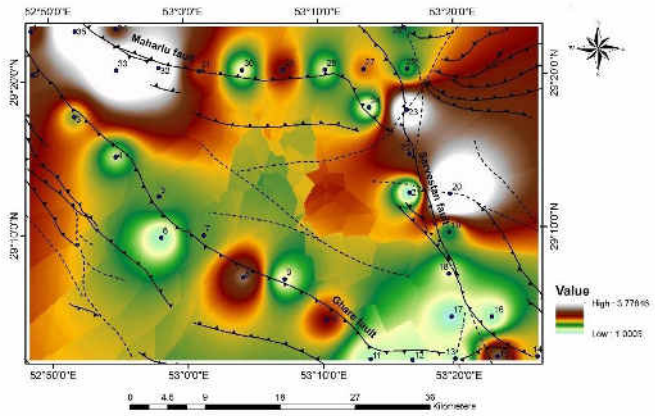

Figure 11: Density distribution map of Smf index values

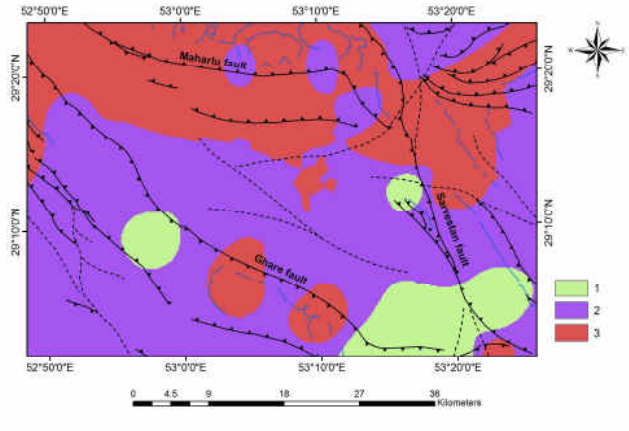

Figure 12: Distribution of Smf classified map

VIII. Asymmetry Factor (AF)

According to Keller and Pinter (1996), Hare and Gardner (1985) the Asymmetry factor is calculated for the area and defined as:

$$Af = \frac{Ar}{At} \times 100$$

Where Ar is the right of the basin stream area and At is the total drainage basin area (El Hamdouni et al., 2008).Af value was calculated along the faults in the sub-basin locations. Table 5 shows the calculated Smf value for all three faults. Finally the Af density distribution map was prepared based on IDW model (Fig, 13). The Af values show range between 11.46 to 90.3 for 45 Sub-basin. The Af amounts were classified based on (El Hamdouni et al., 2008)for understanding the active tectonic variations in the area (Fig, 14). The values classified in three classification: 1 ($|Af-50| > 15$) (high active tectonic), 2 ($|Af-50|$: 7-15) (median active tectonic) and 3 ($|Af-50| < 7$) (low active tectonic) (El Hamdouni et al., 2008). Asymmetry factor is a parameter to indicate tectonic tilting in reaction tectonic activity at the drainage-basin scale (Hare and Gardner, 1985; Keller and Pinter, 2002). This index is sensitive to tilting of vertical on river trend. The values more or less from 50 is possible that be illustrate of tilting (Keller and Pinter, 2002).

Table 5: Values and classes of Af index in the area along Maharlu, Sarvestan and Ghare faults

Maharlu Fault			Sarvestan Fault			Ghare Fault		
No.	AF	Class	*No.*	AF	Class	*No.*	AF	Class
1	75	1	*13*	58.47	2	*24*	60	2
2	41.59	3	*14*	37.18	3	*25*	90.03	1
3	65.89	1	*15*	33.30	3	*26*	65.26	1
4	59.29	2	*16*	18.84	3	*27*	60.10	2
5	42.24	3	*17*	19.43	3	*28*	58.94	2
6	55.20	3	*18*	67.05	1	*29*	11.46	3
7	57.02	2	*19*	68.01	1	*30*	29.81	3
8	79.19	1	*20*	82.58	1	*31*	52.63	3
9	61.35	2	*21*	35.59	3	*32*	88.57	1
10	57.89	2	*22*	57.13	2	*33*	7.81	3
11	43.52	3	*23*	59.25	2	*34*	19.16	3
12	67.45	1				*35*	49.80	3
						36	65.43	1
						37	30.15	3
						38	49.62	3
						39	22.47	3
						40	62.25	2
						41	44.11	3
						42	35.70	3
						43	81.76	1
						44	55.50	3
						45	54.14	3

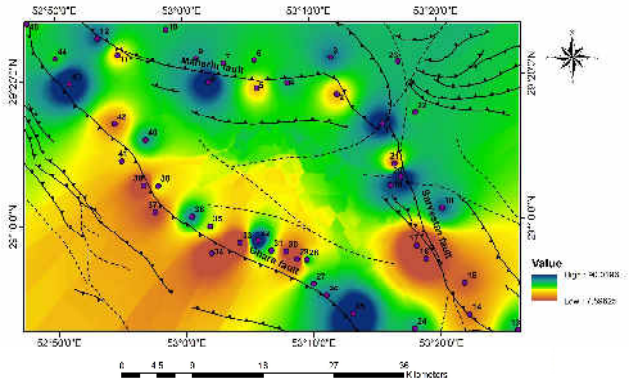

Figure 13: Density distribution map of Af index values

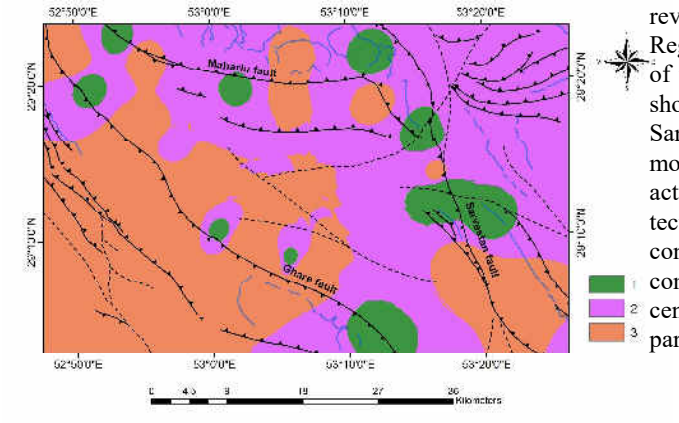

Figure 14: Distribution of Af classified map

IX. Tectonic Activity Map

In this research the potential of tectonic activity in the Maharlu area was presented using geomorphic indices. Density distribution of five morphotectonic indices were determined and all values were classified in three classes based on (El Hamdouni et al., 2008). Relative tectonic activity (Iat) was calculated by average of five geomorphic indices. The Iat values have been classified in four tectonic classification: 1 very high (1<Iat<1.5), 2 high(1.5≤Iat<2), 3 moderate (2≤Iat<2.5); and 4 low (2.5≤Iat) (El Hamdouni et al., 2008). The average classification of five geomorphic indices (Iat) was calculated for different segments of Sarvestan fault, Ghare fault and Maharlu fault as 2.23, 2.53, and 2.48 respectively. Finally the relative tectonic activity map of the study area was drawn with application of fuzzy overlay in Arc GIS (Fig. 15).

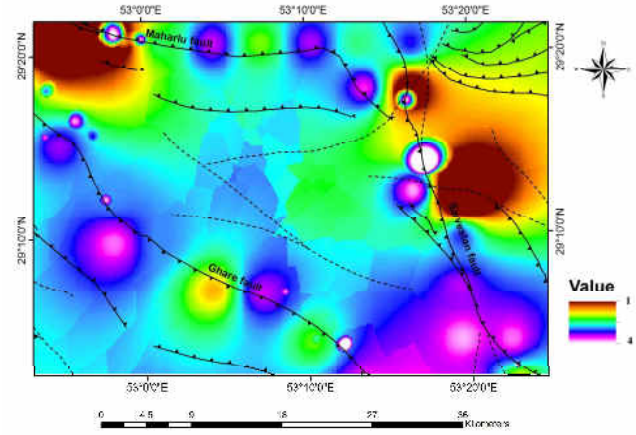

Figure 15: Tectonic activity map of the Maharlu area

X. Conclusion:

The geomorphic indices calculated for assessment of tectonic activity of the Maharlu area. Five geomorphic indices; The stream length-gradient index (Sl), Ratio of valley floor width to valley height (Vf), Index of mountain front sinuosity (Smf), Asymmetry Factor (Af), and Index of Basin shape (Bs) have calculated in this area. Based on the classified values of SL index the study area consists of below tectonic activity. According to the classified values of Smf, Af, and Bs indices and comparison of these values with standard values it can reveal that study area shows moderate tectonic activity. Regarding of the classified values of Vf index and comparison of the results with standard classified values the study area shows low tectonic activity. According to index of Iat values, Sarvestan, Ghare and Maharlu faults show moderate, low and moderate tectonic activity. Results of the amounts of tectonic activity indices (Iat) and overlied data layer show more tectonic activity in the eastern parts and especially in the contacts of Maharlu and Sarvestan faults. Morphotectonic comparisons of faults reveal that the sarvestan fault and the central part of the Ghare faults are more active than other parts of the study are.

References

[1] Alavi, M., 1994, Tectonics of the Zagros orogenic belt of Iran: new data and interpretations: Tectonophysics, v. 229, no. 3-4, p. 211-238.

[2] Andermann, C., and Gloaguen, R., 2009, Estimation of erosion in tectonically active orogenies. Example from the Bhotekoshi catchment, Himalaya (Nepal): International Journal of Remote Sensing, v. 30, no. 12, p. 3075-3096.

[3] Azañón, J., Pérez-Peña, J., Giaconia, F., Booth-Rea, G., Martínez-Martínez, J., and Rodríguez-Peces, M., 2012, Active tectonics in the central and eastern Betic Cordillera through morphotectonic analysis: the case of Sierra Nevada and Sierra Alhamilla: Journal of Iberian Geology, v. 38, no. 1, p. 225-238.

[4] Azor, A., Keller, E. A., and Yeats, R. S., 2002, Geomorphic indicators of active fold growth: South Mountain–Oak Ridge anticline, Ventura basin, southern California: Geological Society of America Bulletin, v. 114, no. 6, p. 745-753.

[5] Berberian, F., Muir, I., Pankhurst, R., and Berberian, M., 1982, Late Cretaceous and early Miocene Andean-type plutonic activity in northern Makran and Central Iran: Journal of the Geological Society, v. 139, no. 5, p. 605-614.

[6] Berberian, M., 1983, The southern Caspian: a compressional depression floored by a trapped, modified oceanic crust: Canadian Journal of Earth Sciences, v. 20, no. 2, p. 163-183.

[7] Berberian, M., 1994, Master "blind" thrust faults hidden under the Zagros folds: active basement tectonics and surface morphotectonics: Tectonophysics, v. 241, no. 3, p. 193-224.

[8] Berberian, M., and King, G., 1981, Towards a paleogeography and tectonic evolution of Iran: Canadian journal of earth sciences, v. 18, no. 2, p. 210-265.

[9] Blanc, E.-P., Allen, M. B., Inger, S., and Hassani, H., 2003, Structural styles in the Zagros simple folded zone, Iran: Journal of the Geological Society, v. 160, no. 3, p. 401-412.

[10] Bull, W. B., and McFadden, L. D., Tectonic geomorphology north and south of the Garlock fault, California, in Proceedings Geomorphology in arid regions. Proceedings of the eighth annual geomorphology symposium. State University of New York, Binghamton1977, p. 115-138.

[11] Burbank, D. W., and Anderson, R. S., 2012, Tectonic geomorphology, John Wiley & Sons.

[12] El Hamdouni, R., Irigaray, C., Fernández, T., Chacón, J., and Keller, E., 2008, Assessment of relative active tectonics, southwest border of the Sierra Nevada (southern Spain): Geomorphology, v. 96, no. 1, p. 150-173.

[13] Falcon, N. L., 1974, Southern Iran: Zagros Mountains: Geological Society, London, Special Publications, v. 4, no. 1, p. 199-211.

[14] Farr, T. G., and Kobrick, M., 2000, Shuttle Radar Topography Mission produces a wealth of data: Eos, Transactions American Geophysical Union, v. 81, no. 48, p. 583-585.

[15] Giaconia, F., Booth-Rea, G., Martínez-Martínez, J. M., Azañón, J. M., Pérez-Peña, J. V., Pérez-Romero, J., and Villegas, I., 2012, Geomorphic evidence of active tectonics in the Sierra Alhamilla (eastern Betics, SE Spain): Geomorphology, v. 145, p. 90-106.

[16] Grohmann, C. H., 2004, Morphometric analysis in geographic information systems: applications of free software GRASS and R: Computers & Geosciences, v. 30, no. 9, p. 1055-1067.

[17] Grohmann, C. H., Riccomini, C., and Alves, F. M., 2007, SRTM-based morphotectonic analysis of the Poços de Caldas Alkaline Massif, southeastern Brazil: Computers & Geosciences, v. 33, no. 1, p. 10-19.

[18] Hare, P. W., and Gardner, T., 1985, Geomorphic indicators of vertical neotectonism along converging plate margins, Nicoya Peninsula, Costa Rica: Allen and Unwin, Boston, p. 75-104.
[19] Jackson, J., and McKenzie, D., 1984, Active tectonics of the Alpine—Himalayan Belt between western Turkey and Pakistan: Geophysical Journal International, v. 77, no. 1, p. 185-264.
[20] Joshi, P. N., Maurya, D., and Chamyal, L., 2013, Morphotectonic segmentation and spatial variability of neotectonic activity along the Narmada–Son Fault, Western India: Remote sensing and GIS analysis: Geomorphology, v. 180, p. 292-306.
[21] Keller, E., and DeVecchio, D., 2012, 5.7 Tectonic Geomorphology of Active Folding and Development of Transverse Drainages.
[22] Keller, E., and Pinter, N., 2002, Earthquakes, uplift, and landscape, New.
[23] Keller, E. A., and Pinter, N., 1996, Active tectonics, Prentice Hall Upper Seddle River, NJ, USA.
[24] Mahmood, S. A., and Gloaguen, R., 2012, Appraisal of active tectonics in Hindu Kush: Insights from DEM derived geomorphic indices and drainage analysis: Geoscience Frontiers, v. 3, no. 4, p. 407-428.
[25] McQuarrie, N., 2004, Crustal scale geometry of the Zagros fold–thrust belt, Iran: Journal of Structural Geology, v. 26, no. 3, p. 519-535.
[26] Navabpour, P., and Barrier, E., 2012, Stress states in the Zagros fold-and-thrust belt from passive margin to collisional tectonic setting: Tectonophysics, v. 581, p. 76-83.
[27] Pérez-Peña, J. V., Azor, A., Azañón, J. M., and Keller, E. A., 2010, Active tectonics in the Sierra Nevada (Betic Cordillera, SE Spain): insights from geomorphic indexes and drainage pattern analysis: Geomorphology, v. 119, no. 1, p. 74-87.
[28] Samani, B., and Faghih, A., 2014, Finite strain analysis in the Seydan anticline using ammonoid spiral shells, Zagros, Iran: Journal of African Earth Sciences, v. 90, p. 25-30.
[29] Sepehr, M., and Cosgrove, J., 2005, Role of the Kazerun Fault Zone in the formation and deformation of the Zagros Fold□Thrust Belt, Iran: Tectonics, v. 24, no. 5.
[30] Silva, P. G., Goy, J., Zazo, C., and Bardajı, T., 2003, Fault-generated mountain fronts in southeast Spain: geomorphologic assessment of tectonic and seismic activity: Geomorphology, v. 50, no. 1, p. 203-225.
[31] Takin, M., 1972, Iranian geology and continental drift in the Middle East: Nature, v. 235, p. 147-150.
[32] Talebian, M., and Jackson, J., 2002, Offset on the Main Recent Fault of NW Iran and implications for the late Cenozoic tectonics of the Arabia–Eurasia collision zone: Geophysical Journal International, v. 150, no. 2, p. 422-439.
[33] Troiani, F., and Della Seta, M., 2008, The use of the Stream Length–Gradient index in morphotectonic analysis of small catchments: A case study from Central Italy: Geomorphology, v. 102, no. 1, p. 159-168.